DYNAMIC AND STATIC TEST OF MODEL PILES OR PILE GROUPS

by

SHINTARO YAO[I)]

SYNOPSIS

The present report is concerned about the results of the experiments where the model piles or pile groups driven into clay layer have been laterally loaded both statically and dynamically.
Following matters are mainly discussed. 1.) Availability and unavailability of static loading test in lateral direction, for the aseismic design concepts. 2.) Influence of pile foundations on the dynamic characteristics of superstructure, in frequency and amplitude. 3.) Dynamical modelling of ground-pile-building system and its simulate calculation.

INTRODUCTION

In the case of pile-supported building which has the basement floor, the base shear forces would be mainly reacted by the underground walls or footing slab surfaces but not so much by pile heads. But in the case of pile-supported building which has no basement floor, the base shear forces would be almost reacted by piles. In such cases, unless the magnitude of seismic loads acting on the pile shafts is correctly estimated, piles could be greatly damaged and these damages might possibly lead to the fatal destruction of the entire building, including the overturning of tall building. There are fairly many cases of buildings supported by bearing piles where upper parts of piles protrude from the ground surface and where there exists void space between the footing slab and the ground surface as pirot'i, resulting from the consolidation settlements of alluvial clay deposit by pumping up. Taking these situations into consideration, the aseismic design philosophy for pile foundations could not be sufficient at present, especially with P.C. piles lacking in ductility.

OUTLINE OF EXPERIMENTS

Testing Apparatus Scheme of the testing apparatus is shown in Fig. 1 and additional explanations are as follows. 1.) At the bottom of clay layer in the soil box, various frequencies of sine waves are transmited through the vibratory table which is equipped with the vibration generator. The soil box has light rotative walls which hold the clay layer in vibratory direction, to avoid both the unnatural confinement of soil movements and the excessive dynamic inertia reactions from rotative walls. 2.) The clay layer is enclosed by the vinyl plastic sheets and glycerin to contain pore water and to cut the frictional resistance between the soil and soil box. 3.) Model piles are aluminous pipes (10.mm diameter. 1.mm thick, Young's modulus $E_p=7.58\times10^5 kg/cm^2$, sectional inertia $I_p=2.89\times10^{-2} cm^4$). 4.) Steel mass and Televibrometer of 31.kg total weight, corresponding to one third of vertical ultimate strength of group piles, are fixed on the footing. 5.) Results of cone tests and vane tests in clay layer are shown in Fig. 2.
Contents of Experiments Contents of experiments are shown in Table 1. as NO.1,2,3,etc..

I) Associate Professor, Division of Architectural Engineering, Shiga Prefectural Junior College, JAPAN

RESULTS OF EXPERIMENTS

Test NO.1 Vertical ultimate bearing capacity is about 9.kg f. per one pile.

Test NO.2 Fig. 3 shows the lateral load-displacement relations obtained at pile-tops in the static tests. Fig. 4 shows the bending strain distributions in depth of each pile where the maximum bending has been observed at the corner pile and the minimum at the center pile. Group effects about displacement and bending moment are recognized in these figures. Comparing these observed bending moments with Chang's solution [1], the lateral coefficient of soil reaction K_h could be estimated and employed as $K_h = 1.0\ kg/cm^3$ in this report.

Test NO.3 Fig. 5 shows the p-δ relation in the lateral direction at the top of rotative walls that hold clay layer. Fig. 6 shows the bending strain distributions of piles just only by the forced shear deformation of clay layer such as in Fig. 5. Bending strains observed here could be considered to be fairly small in the relative importance in seismic interaction.

Test NO.4, NO.5, NO.6 Figs. 7, 8 and 9 show respectively the dynamic response ratio spectra of each single pile obtained from the bending strains and the acceleration measurments. Fig. 10 shows the absolute acceleration spectra in clay layer measured by sensors GA1-GA4.

Test NO.7 Fig.11 shows the dynamic strain distributions along the pile shafts for the typical frequencies (N=5,8,19 and 34 Hz). Fig. 12 shows the dynamic response ratio spectra of each pile. Fig.13 also shows the dynamic response ratio spectra about the acceleration and displacement obtained from the tele-vibrometers that are setted on the footing (TV1) and on the vibratory table (TV2).

Test NO.8 Test situations are the same as those of Test NO.7 except that the level of pile head is G.L.±0. ie.H=0.. Fig.14 shows the dynamic response ratio spectra.

Test NO.9 Fig.15 shows the dynamic response ratio spectra. Fig.16 shows the absolute dynamic axial strain spectra by rocking movements.

SOME CONSIDERATIONS ABOUT EXPERIMENTAL RESULTS

Natural Frequency of Superstructure (N_s) In order to estimate the influence of pile foundation upon the natural frequency of superstructure, a single degree of freedom system for the superstructure is employed, that is : $N_s = \frac{1}{2\pi}\sqrt{\frac{K_s}{W_s}}$, where W_s is the effective mass of superstructure and K_s is the spring constant including the influence of pile foundation. Following equation (1) would be available for estimating the influence of pile foundation upon K_s.

$$\frac{1}{K_s} = \frac{1}{K_p} + \frac{1}{K_b} \qquad (1)$$

where K_p is the spring constant due to pile foundation and K_b is the spring constant of building.

Every observed response spectrum has generally two peaks, one of which coincides with the natural frequency of superstructure including the influence of pile foundation measured in the free vibration test (N_{sm}), and the other of which coincides with the natural frequency of clay layer measured in the free vibration test (N_{gm}).

Now, as shown in Fig. 17, piles are assumed to be free standing on the

perfectly rigid virtual base at the level of - L_m from the ground surface.

Natural frequency of the superstructure in this assumption is calculated as follows (N_{sc}),

$$N_{sc} = \frac{1}{2\pi}\sqrt{\frac{K_p}{W_s}} = \frac{1}{2\pi}\sqrt{\frac{a \cdot E_p \cdot I_p}{(L_m+H)3 \cdot W_s}} \qquad (2)$$

here a=3. when the pile head is hinged, a=12. when the pile head is perfectly rigid and $K_b = \infty$ in these model experiments.

The calculated L_m, which satisfies $N_{sc}=N_{sm}$, could be recognized to be nearly equal to or a little larger than the depth where the maximum bending moment of pile shaft is observed in case of pin-connected pile head. According to these experimental facts and also following to the fact that the ground and piles behave almost identically with each other except the vicinity of pile head, e.g.[2], the author proposes to estimate L_m using Chang's solution [1] as follows,

$$L_m = \frac{1}{\beta} \tan^{-1} \left(\frac{1}{1+2\beta H} \right) \qquad (3)$$

where $\beta = \sqrt[4]{\frac{E_s}{4E_p \cdot I_p}}$, $E_s = K_h \cdot B$, B is the width of pile shaft, H is the protruding length of pile head as shown in Fig. 17.

N_{sc} which is obtained from Eqs. 2 and 3, and N_{sm} which have been measured are shown in Table 2. in comparison.

Natural Frequency of Clay Layer In order to estimate the natural frequency of clay layer, the following examinations 1.) - 5.) have been tried.

1.) From empirical eqations $V_s = 60.q_u^{0.36}$ (m/sec), $q_u = 1/5\ q_c$ where V_s is the shear wave velocity in the ground and $q_c = 3.\ kg/cm^2$ from the cone test results (Fig. 2), the dynamic shear modulus G_s is obtained as follows.

$$G_s = \rho V_s^2 \qquad (4)$$

where ρ is the mass density of the ground.

2.) The natural frequency of elastic layer of thickness H_g for shear translation (N_g) is given by $N_g = V_s/4H_g$. Substituting for this equation the measured natural frequency $N_{gm} = N_g$ ($\doteqdot$ 20 H_z) and H_g (= 54.cm), V_s is obtained, and then from Eq. 4 G_s is obtained.

3.) As illustrated in Fig. 18, the shear translation of clay layer could be modelled as a single degree of freedom system. Then the following equations are obtained.

$$N_{gc} = \frac{1}{2\pi}\sqrt{\frac{K_g}{M_g}} \qquad (5)$$

Where, spring constant of the ground layer K_g is as follows,

$$K_g = \frac{A}{H_g} G_s \qquad (6)$$

and $M_g = \frac{H_g \cdot A}{2 \cdot g} \gamma_s$, A is the sectional area of soil layer and γ_s is the unit weight of soil, refering to Fig. 18.

Equating $N_{gc} = N_{gm}$ in Eq. 5, K_g is obtained, and then G_s is also obtained from Eq. 6.

4.) Searching out the maximum modulus of rigidity from the p-δ relation in Fig. 5, $K_g = \left.\frac{\Delta p}{\Delta \delta}\right|_{max}$ ($\doteqdot$ 833. kg/cm) is obtained, and by Eq. 6

G_s is also obtained.

5.) Using K_h (= 1. kg/cm^3) applied to Chang's solution, G_s would be estimated abbreviately as follows,

$E_s = K_h \cdot B$ = 1. kg/cm^2 , where B = 1. cm. Assuming $E = E_s$,

$$G_s = \frac{E}{2(1+\nu)} \quad (\fallingdotseq 0.36 \text{ kg/cm}^2)$$

where ν is the Poisson's ratio.

G_s, K_g and N_{gc} obtained in the above methods 1.) - 5.) are shown in Table 3.. Methods 1.) - 4.) could be recognized to be fairly reasonable, considering some other relative situations. The result of method 5.) shows that K_h applied to Chang's solution owing to the static test cannot be applied to the dynamic phenomena of the ground.

As a reason of this, the disturbance of clay or the growth of small vacancy between clay and pile surface, by the repeated movement near the ground surface, could be presumed. In Fig. 8 these phenomena could be also observed indirectly comparing with the response before and after resonance.

Vibrating Modes Response spectra could be characterized by the relative magnitude of N_g and N_s as shown in Figs. 7 and 9. Vibrating modes of ground -pile- building system obtained by observing the phases of recorded waves are illustratively shown in Fig. 19 with the characteristic zoning symbols I_s, II_{sg}, III_g, I_g, II_{gs}, III_s in Figs. 7 and 9. In Fig. 19, there are also shown the calculated modes of two-degree of freedom system employing the model which is composed of those shown in Figs. 17 and 18.

Input Shear Forces at Pile Head In order to examine the fundamental seismic input data at pile head, the response amplitude ratio spectra were obtained from the dynamic tests and also from the simulate calculation employing the two-degree of freedom system. The damping ratios h_g of the ground and h_s of the superstructure were employed refering to the observed waves of free vibrating tests. When N_s and N_g are close, the response around resonant frequency shows the drastic increase as shown in Fig. 18.

Axial forces by rocking movements in Fig. 16 are presumed coincidently by the overturning moment calculated from the center of gravity of superstructure and measured accelerations within the limits of $N < N_s$.

Dynamic pile group effect about the shear force distributions at pile heads does not necessarily coincide with the static one as shown in Fig. 12.

CONCLUDING REMARKS

The influence of pile foundation upon the superstructure which has no basement floor, in the earthquake response, could be estimated approximately by Eqs. 1 and 2, and be estimated availably also by the lateral pile -loading tests in site.

The dynamic behavior of the ground-pile-superstructure system could be fundamentally explained by two-degree of freedom system mentioned in this report.

Dynamic characteristics of the ground or of pile group effect cannot be presumed from the static loading test of piles in lateral direction.

REFERENCES

[1] Chang,Y.L. (1937) : Discussion on "Lateral pile- loading Tests" by Feagin, Trans., ASCE, P272-278

[2] Sugimura,Y. (1977) : Earthquake Observation and Dynamic Analysis of a Building Supported on Long Piles, Proc. of 6th WCEE, VOL.II, P1570-1575

Table 1. Contents of Experiments

Test NO.	Pile	H (cm)	W_b g(kg)	Loading	Measurement
NO.1	9Gr.Pin.& Single P.	6.	-	Static	Axial forces Settlements
NO.2	do.	6.	-	Static	Bending strains Displacements
NO.3	9Gr.Pin.	6.	-	Static	do.
NO.4	Single p.	7.7	3.1	Dynamic	Dynamic spectra Natural freq.
NO.5	do.	4.9	0.63	Dynamic	do.
NO.6	do.	3.8	0.31	Dynamic	do.
NO.7	9Gr.Pin.	6.	31.	Dynamic	do.
NO.8	do.	0.	31.	Dynamic	do.
NO.9	9Gr.Fix.	0.	31.	Dynamic	do.

notes; H, W_b : shown in Fig.17
9Gr. : 3 x 3 Group Piles
Pin. : Pin-connected at Pile Head
Fix. : Fixed at Pile Head

Table 2. Measured and Calculated N_s

Test NO.	N_{sm}(Hz)	N_{sc}(Hz)
NO.4	10.	11.3
NO.5	23.	28.8
NO.6	40.	42.7
NO.7	8.5	11.7
NO.8	13.5	13.9
NO.9	22.	27.7

Table 3. Examined Results for Clay Layer

Examined method	G_s(kg/cm^2)	K_g(kg/cm)	N_{gc}(Hz)
1.)	41.8	2939.	21.1
2.)	33.	2320.	18.8
3.)	37.6	2640.	20.
4.)	29.	2039.	17.6
5.)	0.36	25.3	2.

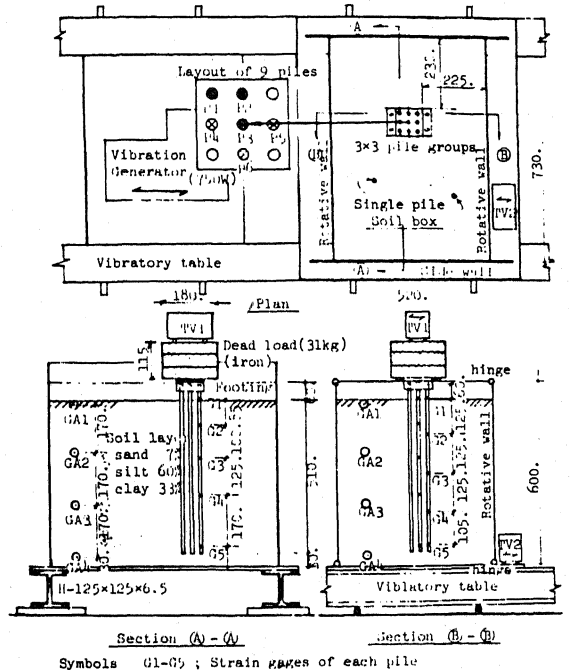

Symbols G1-G9 ; Strain gages of each pile
GA1-GA4 ; Accelerometers in soil layer
TV1,TV2 ; Tele-Vibrometer (acceleration & displacement)

Fig. 1 Scheme of Testing Apparatus

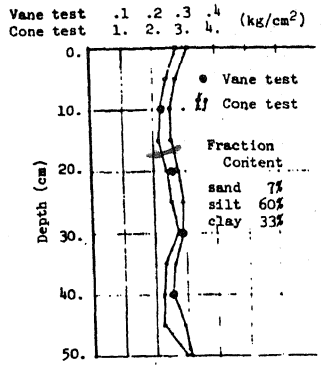

Fig. 2 Soil profile

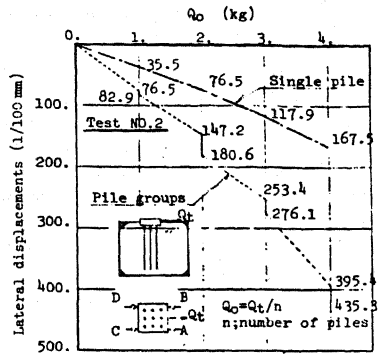

Fig. 3 Lateral loading test

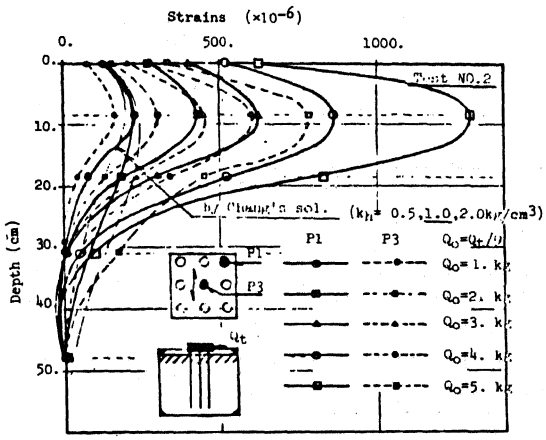

Fig. 4 Bending strain distributions in static test

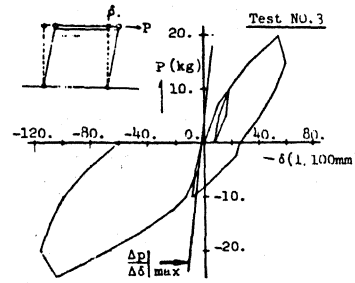

Fig. 5 Lateral load(p)-displacement(δ) relation at the top of rotative wall

Damping factors are evaluated in two cases as ① $h_G=\frac{18.}{2\pi N_G}$, $h_S=\frac{18.}{2\pi N_S}$ and ② $h_G=\frac{24.}{2\pi N_G}$, $h_S=\frac{24.}{2\pi N_S}$ in Figs. 7,8 and 9.

a_t is the acceleration evaluated from the strain of G1 at the level of ground surface.
a_b is the acceleration measured by GA4 at the bottom of soil layer.

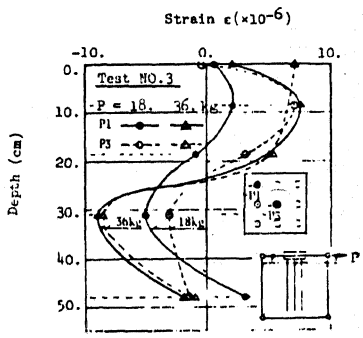

Fig. 6 Bending strain distributions of piles when rotative wall is laterally loaded by P at the top

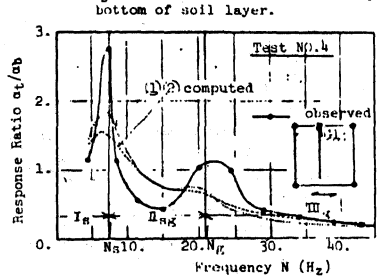

Fig. 7 Acceleration response ratio spectra

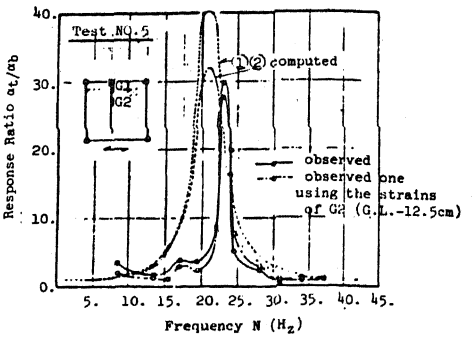

Fig. 8 Acceleration response ratio spectra

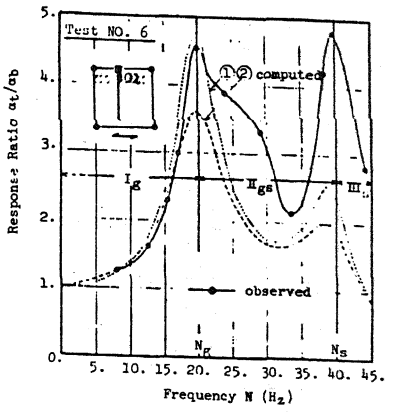

Fig. 9 Acceleration response ratio spectra

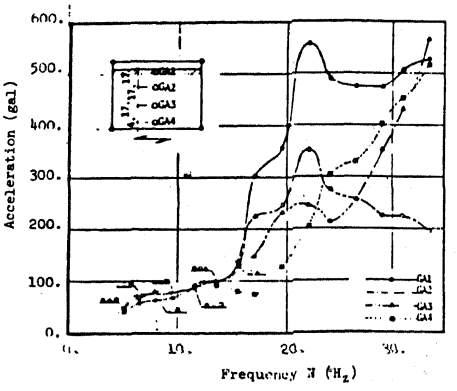

Fig. 10 Absolute acceleration spectra in soil layer

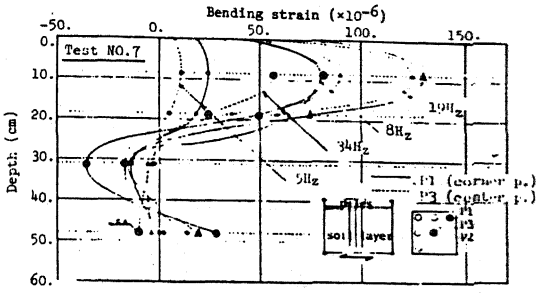

Fig. 11 Bending strain distributions along pile shafts obtained in dynamic tests

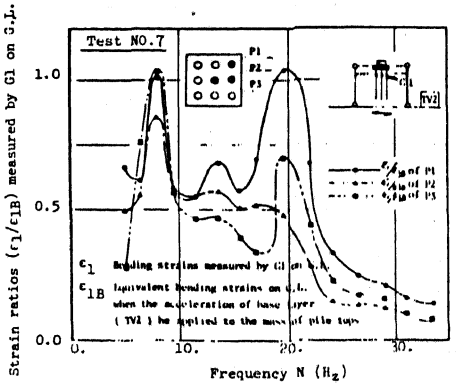

Fig. 12 Strain ratio spectra

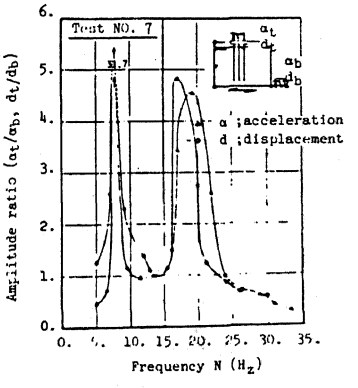

Fig. 13 Amplitude ratio spectra by Tele-Vibrometers TV1&TV2

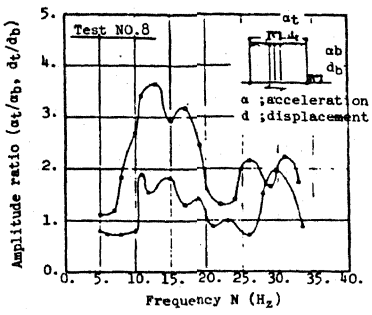

Fig. 14 Amplitude ratio spectra by Tele-Vibrometers TV1,TV2

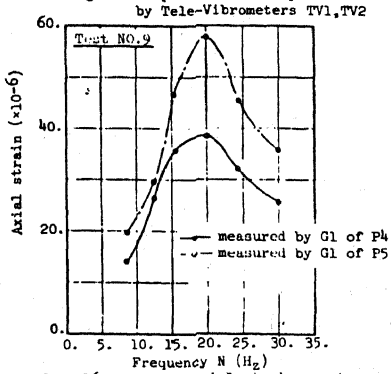

Fig. 16 Absolute axial strain spectra by rocking movement

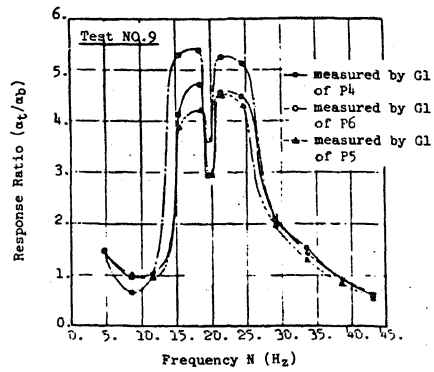

Fig. 15 Acceleration response ratio spectra

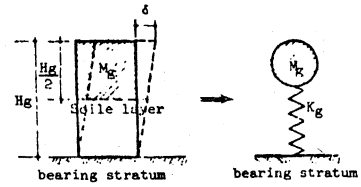

Fig. 18 Modelling of the ground

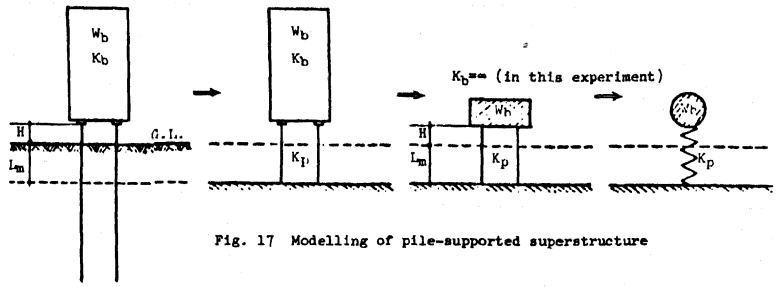

Fig. 17 Modelling of pile-supported superstructure

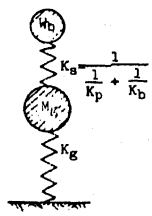

Two-degree of freedom system, composed of the models shown in Figs. 17 and 18.

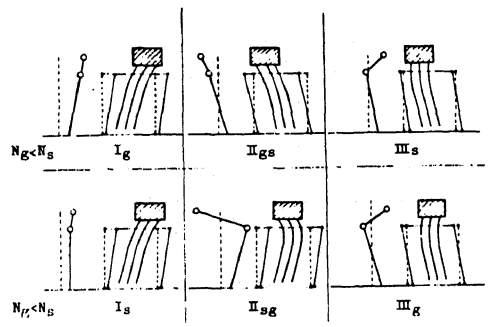

Fig. 19 Scheme of observed and computed modes